Quasiclassical magnetic order and its loss in a spin-$\frac{1}{2}$ Heisenberg antiferromagnet on a triangular lattice with competing bonds

P. H. Y. Li* and R. F. Bishop†
School of Physics and Astronomy, Schuster Building, University of Manchester, Manchester M13 9PL, UK

C. E. Campbell
School of Physics and Astronomy, University of Minnesota, 116 Church Street SE, Minneapolis, Minnesota 55455, USA

(Received 22 October 2014; published 22 January 2015)

We use the coupled cluster method (CCM) to study the zero-temperature ground-state (GS) properties of a spin-$\frac{1}{2}$ $J_1 - J_2$ Heisenberg antiferromagnet on a triangular lattice with competing nearest-neighbor and next-nearest-neighbor exchange couplings $J_1 > 0$ and $J_2 \equiv \kappa J_1 > 0$, respectively, in the window $0 \leqslant \kappa < 1$. The classical version of the model has a single GS phase transition at $\kappa^{\rm cl} = \frac{1}{8}$ in this window from a phase with 3-sublattice antiferromagnetic (AFM) 120° Néel order for $\kappa < \kappa^{\rm cl}$ to an infinitely degenerate family of 4-sublattice AFM Néel phases for $\kappa > \kappa^{\rm cl}$. This classical accidental degeneracy is lifted by quantum fluctuations, which favor a 2-sublattice AFM striped phase. For the quantum model we work directly in the thermodynamic limit of an infinite number of spins, with no consequent need for any finite-size scaling analysis of our results. We perform high-order CCM calculations within a well-controlled hierarchy of approximations, which we show how to extrapolate to the exact limit. In this way we find results for the case $\kappa = 0$ of the spin-$\frac{1}{2}$ model for the GS energy per spin, $E/N = -0.5521(2)J_1$, and the GS magnetic order parameter, $M = 0.198(5)$ (in units where the classical value is $M^{\rm cl} = \frac{1}{2}$), which are among the best available. For the spin-$\frac{1}{2}$ $J_1 - J_2$ model we find that the classical transition at $\kappa = \kappa^{\rm cl}$ is split into two quantum phase transitions at $\kappa_1^c = 0.060(10)$ and $\kappa_2^c = 0.165(5)$. The two quasiclassical AFM states (viz., the 120° Néel state and the striped state) are found to be the stable GS phases in the regime $\kappa < \kappa_1^c$ and $\kappa > \kappa_2^c$, respectively, while in the intermediate regimes $\kappa_1^c < \kappa < \kappa_2^c$ the stable GS phase has no evident long-range magnetic order.

DOI: 10.1103/PhysRevB.91.014426 PACS number(s): 75.10.Jm, 75.30.Kz, 75.50.Ee, 75.30.Cr

I. INTRODUCTION

Quantum Heisenberg antiferromagnets (HAFMs), comprising spins (with spin quantum number s) on an infinite regular lattice in two spatial dimensions, and interacting via a pure nearest-neighbor (NN) Heisenberg potential with exchange coupling $J_1 > 0$, have long occupied a special role in the theory of quantum phase transitions. Thus, for example, the well-known Mermin-Wagner theorem [1] proves that in both one and two dimensions HAFMs are disordered at any nonzero temperature ($T \neq 0$), in the sense that thermal fluctuations completely destroy all long-range order (LRO). Similarly, in one dimension quantum fluctuations destroy the Néel LRO even at zero temperature ($T = 0$). On the other hand, the Mermin-Wagner theorem does not prohibit a ground state (GS) with LRO for any two-dimensional (2D) model with a continuous symmetry.

It thus remains an open question as to whether a particular 2D spin-lattice model will or will not display LRO in its GS at $T = 0$. For a pure 2D HAFM both quantum fluctuations and any geometrical frustration present in the lattice can potentially combine to destroy long-range Néel-type order. Quantum fluctuations are generally larger for smaller values of s, stronger frustration, and lower coordination number z. Of the 11 uniform Archimedean lattices, those tilings with the greatest frustration are the triangular lattice (with $z = 6$) and the kagome lattice (with $z = 4$). Thus, the spin-$\frac{1}{2}$ HAFMs on the triangular and kagome lattices have attracted much specific interest in the past.

For the triangular-lattice HAFM the classical ($s \to \infty$) GS is a 3-sublattice Néel state with an angle of 120° between the spins on different sublattices, which thus breaks the translational symmetry of the lattice. Historically, some 40 years ago, the spin-$\frac{1}{2}$ HAFM on the triangular lattice was the first model to be proposed [2,3] as a microscopic realization of a system whose GS might be a quantum spin liquid (QSL). It was argued that the GS might be similar to that of the 1D HAFM, and it was thus proposed that it had the form of a rotationally invariant, resonating valence bond (RVB) state, instead of a quasiclassical Néel state akin to the exact classical GS, albeit with a reduced (but nonzero) value of the corresponding sublattice magnetic order parameter.

By contrast, spin-wave theory (SWT) [4–9] results even at higher orders consistently predict that quantum fluctuations on the spin-$\frac{1}{2}$ triangular-lattice HAFM do not destroy the 120° Néel antiferromagnetic (AFM) LRO, but lead to a reduction in the sublattice magnetization of around 50% from the classical value. A number of variational calculations have also been performed for the spin-$\frac{1}{2}$ triangular-lattice HAFM with conflicting results. While some calculations [10,11] predict a quasiclassical ordered state, others [12–14] predict a magnetically disordered state. Typically, however, the former are based on variational wave functions with LRO built in from the outset, while the latter typically employ a spin-liquid type of wave function.

While many of the early numerical studies [15–19] for the spin-$\frac{1}{2}$ triangular-lattice HAFM based on the exact diagonalization (ED) of small lattice clusters predicted a GS

*peggyhyli@gmail.com
†raymond.bishop@manchester.ac.uk

with no, or very small, magnetic LRO, it was later pointed out rather forcefully [20] that two basic requirements need to be carefully met in order to analyze the raw numerical ED data properly. First, a consistent finite-size scaling analysis is needed to reach the thermodynamic limit ($N \to \infty$) of a lattice with N spins, and second, a proper quantum definition of observables needs to be made. Bernu *et al.* [20] argued that once those two constraints are met, the numerical data point to an ordered ground state for the infinite lattice. It is clear that the $N \to \infty$ extrapolation is rather difficult for this model. In a separate paper [21] Bernu *et al.* quote an extrapolated ED value for the magnetic order parameter M of approximately 50% of the classical value with a large error, probably of the order of $\pm 5\%$ or more. This is in reasonable agreement with the corresponding predictions of $M = 47.74\%$ and 49.95% of the classical value from leading-order SWT and second-order SWT, respectively [9], in which M is correct to order $O(1/s)$ and $O(1/s^2)$, respectively, in the usual SWT $1/s$ expansion. A more recent ED analysis [22] quotes a more accurate, reduced value for M of 38.6% of the classical value.

Series expansion (SE) methods constructed around an ordered state have given equally confusing results for the spin-$\frac{1}{2}$ triangular lattice HAFM. For example, an early $T = 0$ SE calculation [23] found some evidence that this model may be very close to a quantum critical point (QCP). If ordered at all, the model was estimated to have a value for M much smaller than the SWT estimates, and rather close to zero. By contrast, a much more recent SE study [24] quoted a value for M of $(38 \pm 4)\%$ of the classical value.

We turn finally to other recent calculations for the spin-$\frac{1}{2}$ triangular-lattice HAFM, employing state-of-the-art tools of microscopic quantum many-body theory. First, sequences of clusters, using pinning fields and cylindrical boundary conditions to provide for rapidly converging finite-size scaling ($N \to \infty$), have been studied using the density-matrix renormalization group (DMRG) method [25]. Nevertheless, it was found that the finite-size analysis for the triangular lattice HAFM was much less accurate than that for the corresponding HAFM on the square lattice, for example. The best result thus obtained for the magnetic order parameter of the spin-$\frac{1}{2}$ triangular lattice HAFM is $M \approx (41 \pm 3)\%$ of the classical value. Second, the spin-$\frac{1}{2}$ triangular lattice HAFM has also been studied on clusters of up to $N = 144$ sites using the Green's function Monte Carlo (GFMC) method [26], together with a stochastic reconfiguration technique that allows the fixed-node approximation (which is needed to overcome the well-known minus-sign problem) to be released in a controlled, albeit approximate, way. The best estimate thus obtained in the thermodynamic limit ($N \to \infty$) for the magnetic order parameter of the spin-$\frac{1}{2}$ triangular lattice HAFM is $M \approx (41 \pm 2)\%$ of the classical value. It is perhaps worth noting in this context that an earlier fixed-node GFMC calculation [27] of the model gave a much less accurate value for the order parameter M as large as 62% of the classical value.

Finally, we note that the coupled cluster method (CCM), which will be employed in the present study, has also been previously been applied to the spin-$\frac{1}{2}$ triangular lattice HAFM [28–31]. As will be explained in more detail in Sec. III, the CCM is a size-extensive method that deals with infinite lattices ($N \to \infty$) from the outset. Nevertheless, results are obtained at various levels of truncation in a well-defined and systematic sequence of hierarchical approximations, namely the lattice-animal-based subsystem (LSUBm) scheme described in Sec. III. The only approximation then made is to extrapolate to the exact limit $m \to \infty$ of the truncation index m. The earliest CCM results [28,29] were based on relatively low-order approximations with $2 \leqslant m \leqslant 6$, and gave an extrapolated result for the order parameter of the spin-$\frac{1}{2}$ triangular lattice HAFM of $M \approx 51\%$ of the classical value. Later results based on more accurate extrapolations with $2 \leqslant m \leqslant 8$ [30] and $4 \leqslant m \leqslant 10$ [31] gave much improved results of $M \approx 42.7\%$ and 37.3% of the classical value, respectively. Both are in excellent agreement with the corresponding results using the DMRG [25], GFMC [26], ED [22], and SE [24] methods.

Thus, by now, there is a rather clear consensus that the spin-$\frac{1}{2}$ HAFM on the triangular lattice retains the 3-sublattice 120° Néel ordering of the classical ($s \to \infty$) version of the model, albeit with a significant decrease in the magnetic order parameter M to a value of around $(40 \pm 2)\%$ of the classical value, due to quantum fluctuations. Nevertheless, the model retains interest, both experimentally and theoretically. On the experimental side it is now believed that the spin-$\frac{1}{2}$ HAFM on the triangular lattice can rather accurately be realized in the compound $Ba_3CoSb_2O_9$ [32,33], in which the magnetic Co^{2+} ions form uniform triangular lattice layers. In this compound the effective magnetic moment of the Co^{2+} ions, which possess true spin $s = \frac{3}{2}$, can be well described by an $s = \frac{1}{2}$ pseudospin at low enough temperatures T (such that $k_B T$ is much smaller than the spin-orbit coupling), where the magnetic properties are determined by the lowest Kramers doublet. Unlike in earlier possible realizations of spin-$\frac{1}{2}$ triangular lattice HAFMs, such as Cs_2CuCl_4 [34] and Cs_2CuBr_4 [35,36], in which the triangular lattice is spatially distorted, and thus with an exchange interaction that is spatially anisotropic, the triangular lattice in $Ba_3CoSb_2O_9$ is expected to be regular.

On the theoretical side the spin-$\frac{1}{2}$ triangular lattice HAFM retains specific interest as a starting-point to consider ways of extending the model to investigate the stability of the classical 120° 3-sublattice Néel order against applied perturbations. We know, in particular, that exotic (nonclassical) nonmagnetically ordered states for spin-lattice systems tend to be favored quantum-mechanically in situations for which the classical ($s \to \infty$) counterpart has two or more different forms of GS ordering that are degenerate in energy. At the classical level Villain *et al.* [37] showed how thermal fluctuations could select, through the so-called *order-by-disorder* mechanism, a specific form of order, which has softer excitation modes and hence, for a given low energy, a larger density of states and a larger entropy.

The commonest cause of such classical GS degeneracy is when competing interactions are present. One such example is the so-called $J_1 - J_2$ model on the triangular lattice in which the NN interactions with exchange coupling strength $J_1 > 0$ now compete with next-nearest-neighbor (NNN) interactions with exchange coupling strength $J_2 \equiv \kappa J_1 > 0$. We are thus led to the study of a model in which both geometric and dynamic forms of frustration are present simultaneously. In the present paper we will consider this model for spins with $s = \frac{1}{2}$. Although initial interest will focus on determining the

critical value κ_1^c of the frustration parameter κ at which the 120° Néel order vanishes, our overall aim here is to study the entire ($T = 0$) GS phase diagram of the spin-$\frac{1}{2}$ $J_1 - J_2$ model on the triangular lattice in the range $0 \leqslant \kappa \leqslant 1$ of the frustration parameter, in the case $J_1 > 0$.

Since the CCM has been shown to describe very accurately the limiting case of the model when $\kappa = 0$, as discussed above, we shall employ it here also when $\kappa \neq 0$. The plan of the rest of the paper is as follows. The model itself is first discussed in Sec. II, where we also discuss its classical ($s \to \infty$) limit. The main elements of the CCM are then reviewed in Sec. III, before presenting our results in Sec. IV. We end with a summary and discussion in Sec. V.

II. THE MODEL

The Hamiltonian of the $J_1 - J_2$ model on the triangular lattice is given by

$$H = J_1 \sum_{\langle i,j \rangle} \mathbf{s}_i \cdot \mathbf{s}_j + J_2 \sum_{\langle\langle i,k \rangle\rangle} \mathbf{s}_i \cdot \mathbf{s}_k, \tag{1}$$

where index i runs over all triangular lattice sites, and indices j and k run over all NN and NNN sites to i, respectively, counting each bond once and once only. Each lattice site i carries a particle with spin $s = \frac{1}{2}$ and a spin operator $\mathbf{s}_i = (s_i^x, s_i^y, s_i^z)$. The lattice and exchange bonds are illustrated in Fig. 1(a). We consider the case where both the NN and NNN bonds are antiferromagnetic (i.e., $J_1 > 0$ and $J_2 \equiv \kappa J_1 > 0$). Henceforth, with no loss of generality, we set $J_1 \equiv 1$ to set the overall energy scale.

The classical ($s \to \infty$) version of the model has been discussed in some detail by Jolicoeur *et al.* [38]. They showed that the 3-sublattice 120° Néel antiferromagnetic (AFM) state illustrated in Fig. 1(b) exists for $\kappa \leqslant \kappa_1^{\rm cl} = \frac{1}{8}$. This state thus has an energy per spin, E/N, given by

$$\frac{E_{\rm Néel}}{Ns^2} = 3\left(\kappa - \frac{1}{2}\right). \tag{2}$$

At $\kappa = \kappa_1^{\rm cl}$ the system then undergoes a first-order phase transition into an infinitely degenerate family (IDF) of 4-sublattice Néel ground states illustrated in Fig. 1(c), in which the only constraint is $\mathbf{s}_A + \mathbf{s}_B + \mathbf{s}_C + \mathbf{s}_D = 0$, where $\mathbf{s}_i$ denotes the spin on each of the four sublattices, $i = A, B, C, D$, as shown. Each member of this IDF has an energy per spin given by

$$\frac{E_{\rm IDF}}{Ns^2} = -\kappa - 1. \tag{3}$$

This IDF of 4-sublattice Néel states was shown to form the stable GS phase for $\kappa_1^{\rm cl} \leqslant \kappa \leqslant \kappa_2^{\rm cl} = 1$. At $\kappa = \kappa_2^{\rm cl}$ the system then undergoes a second-order phase transition to an incommensurate spiral phase with energy per spin given by

$$\frac{E_{\rm spiral}}{Ns^2} = -\frac{1}{2}\left(3\kappa + \frac{1}{\kappa}\right). \tag{4}$$

This state persists for all values $\kappa > \kappa_2^{\rm cl}$. In the limiting case $\kappa \to \infty$, when the NN interactions no longer contribute, the three sublattices effectively decouple and each of them again has a 120° Néel configuration of spins.

The immediate question that arises is whether quantum fluctuations will lift the degeneracy of the classical IDF of states in the regime $\frac{1}{8} < \kappa < 1$, by the order-by-disorder mechanism. Thus, it is well known that any accidental degeneracy that occurs in systems that have continuous degrees of freedom is usually removed by either thermal or quantum fluctuations [37,39–41]. Various authors [38,42,43] have applied lowest-order [i.e., to $O(1/s)$] SWT and shown that to this order the 2-sublattice striped states, one of which is illustrated in Fig. 1(d), are energetically preferred among the IDF family. Korshunov [39] also asserts that thermal fluctuations at the classical level favor the same collinear striped ordering as do quantum fluctuations. ED calculations on finite clusters [44] also led credence to this finding. The striped AFM states have ferromagnetic ordering along one direction [viz., the horizontal one in Fig. 1(d)] and AFM ordering along the other two principal directions of the triangular lattice. They are thus threefold-degenerate and break the rotational invariance of the system.

Various authors [38,42–52] have studied the spin-$\frac{1}{2}$ version of the $J_1 - J_2$ model on the triangular lattice, using a number of approximate methods, with little consensus to date concerning the $T = 0$ GS phase diagram. On the other hand, to the best of our knowledge, no high-order, systematically improvable method has yet been applied to this spin-$\frac{1}{2}$ model. It is our aim here to apply one such technique, namely the CCM, to the model, in the regime $0 \leqslant \kappa \leqslant 1$ of most interest.

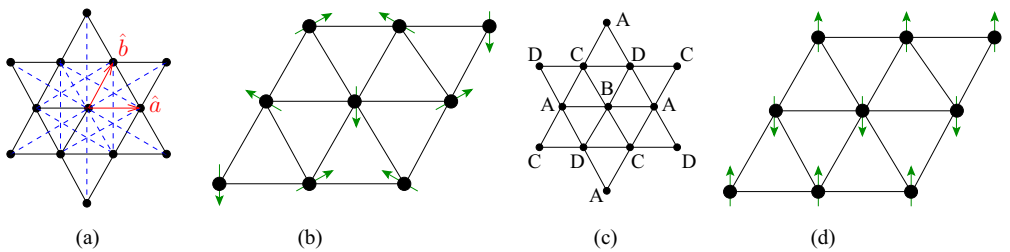

FIG. 1. (Color online) The $J_1 - J_2$ model on the triangular lattice with $J_1 > 0$ and $J_2 > 0$, showing (a) the bonds ($J_1 \equiv$ black solid lines; $J_2 \equiv$ blue dashed lines) and the Bravais lattice vectors $\hat{a}$ and $\hat{b}$; (b) the 120° Néel antiferromagnetic (AFM) state; (c) the infinitely degenerate family of classical 4-sublattice ground states on which the spins on the same lattice are parallel to each other, with the sole constraint that the sum of four spins on different sublattices is zero; and (d) one of the three degenerate striped AFM states. For the two states shown the arrows represent the directions of the spins located on lattice sites ●.

III. THE COUPLED CLUSTER METHOD

The CCM (see, e.g., Refs. [28,53–62] and references cited therein) is one of the most powerful and most versatile techniques of modern quantum many-body theory. Among applications in a great variety of fields in physics and chemistry, it has, in particular, been applied with considerable success to a large number of spin-lattice problems in quantum magnetism (see, e.g., Refs. [28–31,55,58–81] and references cited therein). The CCM is especially suitable for the study of frustrated magnetic systems for which the main alternative techniques are often limited in their applicability. For example, quantum Monte Carlo (QMC) methods are usually severely restricted in such cases by the well-known "minus-sign problem." Similarly, the ED of finite lattice clusters is limited in practice to such relatively small clusters that it can be rather insensitive to the details of some subtle forms of phase order that might be present. By contrast to almost all of the alternative methods that are capable of systematic improvement within well-defined hierarchical approximation schemes, the CCM provides both a size-consistent and size-extensive technique, which gives results from the outset in the thermodynamic (infinite-lattice, $N \to \infty$) limit, with no need, therefore, for any finite-size scaling of the results.

We now briefly outline the CCM methodology to solve the GS Schrödinger ket- and bra-state equations,

$$H|\Psi\rangle = E|\Psi\rangle, \quad \langle\tilde{\Psi}|H = E\langle\tilde{\Psi}|. \tag{5}$$

In order to describe quantitatively the quantum correlations present in the exact GS phase under study, in the CCM one refers them to a suitable, normalized model (or reference) state $|\Phi\rangle$. This state is required only to be a fiducial vector (or generalized vacuum state) with respect to a suitable set of mutually commuting, many-particle creation operators C_I^+. Here, the index I is a set-index that defines a multiparticle configuration, and the requirement is that the set of states $\{C_I^+|\Phi\rangle\}$ completely span the ket-state Hilbert space.

A key element of the CCM is that, unlike in the configuration-interaction method, in which the decomposition of $|\Psi\rangle$ is made linearly in this set, it is now made in an exponentiated form. Specifically, we have the parametrizations

$$|\Psi\rangle = e^S|\Phi\rangle, \quad \langle\tilde{\Psi}| = \langle\Phi|\tilde{S}e^{-S}, \tag{6}$$

where the two correlation operators S and $\tilde{S}$ are formally decomposed as follows,

$$S = \sum_{I\neq 0} \mathcal{S}_I C_I^+, \quad \tilde{S} = 1 + \sum_{I\neq 0} \tilde{\mathcal{S}}_I C_I^-, \tag{7}$$

where we define $C_0^+ \equiv 1$ to be the identity operator, and $C_I^- \equiv (C_I^+)^\dagger$. For the case of spin-lattice problems of the type considered here the set-index I simply represents any subset of the entire set of lattice sites (with possible repeats of any site indices), as discussed more fully below. It denotes a multispin-flip configuration with respect to the model state $|\Phi\rangle$, with $C_I^+|\Phi\rangle$ representing the corresponding wave function associated with this configuration of spins. Hence, the operators $\{C_I^+\}$ and $\{C_I^-\}$ are sets of mutually commuting creation and destructor operators, respectively, defined with respect to the state $|\Phi\rangle$ taken as a (generalized vacuum) reference state. They are hence chosen to obey the respective relations

$$\langle\Phi|C_I^+ = 0 = C_I^-|\Phi\rangle, \quad \forall I \neq 0. \tag{8}$$

By construction, therefore, the states defined by Eqs. (6) and (7) obey the normalization conditions $\langle\tilde{\Psi}|\Psi\rangle = \langle\Phi|\Psi\rangle = \langle\Phi|\Phi\rangle = 1$.

In order both to treat each lattice site on an equal footing and to make the computational implementation of the technique as universal as possible, it is very convenient to make a passive rotation of the spin on each lattice site in each model state $|\Phi\rangle$ so that in its own local spin-coordinate frame it points along the negative z axis, which we henceforth denote as the downward direction. Such passive rotations are canonical transformations that leave the underlying SU(2) commutation relations unchanged, and which, therefore, have no physically observable consequences. In these local spin coordinates, which are clearly unique to each model state, every model state then takes the universal form $|\Phi\rangle = |\downarrow\downarrow\downarrow\cdots\downarrow\rangle$, and the Hamiltonian has to be rewritten accordingly in these spin coordinates. Similarly, in these local spin-coordinate frames, C_I^+ takes a universal form, $C_I^+ \to s_{l_1}^+ s_{l_2}^+ \cdots s_{l_n}^+$, a product of single-spin raising operators, $s_l^+ \equiv s_l^x + i s_l^y$. The set index $I \to \{l_1,l_2,\ldots,l_n;\ n = 1,2,\ldots,2sN\}$ thus simply becomes a set of (possibly repeated) lattice site indices, where $N(\to\infty)$ is the total number of sites. In the case of an arbitrary spin quantum number s, a spin raising operator s_l^+ can be applied a maximum number of $2s$ times, on a given site l. Hence, in any set index I included in the expansions of Eq. (7) a given site l may appear no more than $2s$ times. Hence, in the present case where $s = \frac{1}{2}$, each site index l_j included in any single set index I may appear no more than once.

The (formally complete) set of GS multispin c-number correlation coefficients $\{\mathcal{S}_I,\tilde{\mathcal{S}}_I\}$ is now determined by requiring that the GS energy expectation functional,

$$\bar{H} = \bar{H}\{\mathcal{S}_I,\tilde{\mathcal{S}}_I\} \equiv \langle\Phi|\tilde{S}e^{-S}He^S|\Phi\rangle, \tag{9}$$

is minimized with respect to each of the coefficients $\{\mathcal{S}_I,\tilde{\mathcal{S}}_I\,;\forall I \neq 0.\}$. From Eqs. (7) and (9) we thus obtain the coupled sets of equations,

$$\langle\Phi|C_I^- e^{-S}He^S|\Phi\rangle = 0, \quad \forall I \neq 0, \tag{10}$$

by minimizing with respect to the parameter $\tilde{\mathcal{S}}_I$, and

$$\langle\Phi|\tilde{S}e^{-S}[H,C_I^+]e^S|\Phi\rangle, \quad \forall I \neq 0, \tag{11}$$

by minimizing with respect to the parameter $\mathcal{S}_I$. Equation (10) takes the form of a coupled set of nonlinear multinomial equations for the set of creation parameters $\{\mathcal{S}_I\}$. Once solved the parameters $\{\mathcal{S}_I\}$ are used as input to the coupled set of linear equations for the set of destruction parameters $\{\tilde{\mathcal{S}}_I\}$, given by Eq. (11). Once Eq. (10) has been satisfied, the value of $\bar{H}$ at the minimum, which is simply the GS energy, may be expressed in the form

$$E = \langle\Phi|e^{-S}He^S|\Phi\rangle = \langle\Phi|He^S|\Phi\rangle. \tag{12}$$

Equation (11) for the destruction parameters $\{\tilde{\mathcal{S}}_I\}$ may then also be written in the equivalent form of a set of generalized eigenvalue equations,

$$\langle\Phi|\tilde{S}(e^{-S}He^S - E)C_I^+|\Phi\rangle, \quad \forall I \neq 0. \tag{13}$$

Another key feature of the CCM is that although the operator S is exponentiated, the actual equations (10) and (13) that we solve are automatically of finite order in the coefficients $\{\mathcal{S}_I\}$, thereby obviating the need for any artificial truncation. The reason is that in Eqs. (10) and (13) the operator S only appears in the combination $e^{-S}He^{S}$, a similarity transformation of the Hamiltonian. This form may be exactly and simply expanded as the well-known nested commutator sum. This otherwise infinite sum then terminates exactly with the double-commutator term, first because all of the terms comprising S in its expansion of Eq. (7) commute with one another and are just simple products of single spin-raising operators as described above, and second because of the basic SU(2) commutation relations (and see, e.g., Refs. [28,29,58] for further details). Exact such terminations equally apply for the GS expectation values of all physical observables. One such, in which we will be interested, is the magnetic order parameter, defined to be the average local on-site magnetization,

$$M \equiv -\frac{1}{N}\langle\tilde{\Psi}|\sum_{l=1}^{N} s_l^z|\Psi\rangle = -\frac{1}{N}\langle\Phi|\tilde{S}\sum_{l=1}^{N} e^{-S}s_l^z e^{S}|\Phi\rangle, \quad (14)$$

where s_l^z is defined now with respect to the chosen local spin-coordinate frame on lattice site l, for the particular model state $|\Phi\rangle$ being employed.

Thus, for the reasons stated above, the only approximation made in a practical implementation of the CCM is to truncate the set of indices $\{I\}$ in the expansions of the correlation operators S and $\tilde{S}$ in Eq. (7). It is worth noting in this context that it may be shown [57] that the CCM exactly obeys both the Goldstone linked cluster theorem (and hence size extensivity) and the important Hellmann-Feynman theorem at any such level of truncation. We use here the well-tested (lattice-animal-based subsystem) LSUBm scheme [28–31,55,58–81] in which, at the mth level of approximation, one retains all multispin-flip configurations I that are defined over no more than m contiguous lattice sites. Any multispin-flip configuration or cluster is defined to be contiguous if every site is NN to at least one other in the cluster. The number, N_f, of such distinct fundamental configurations is reduced by fully exploiting the space- and point-group symmetries, as well as any conservation laws, that pertain to both the Hamiltonian and the model state being used. Nevertheless, N_f increases rapidly as the LSUBm truncation index m is increased, and it becomes necessary at the higher orders to use massive parallelization together with supercomputing resources [28,82]. In the present work we employ both the 120° Néel and the collinear striped AFM states shown in Figs. 1(b) and 1(d), respectively, as CCM model states, and we have been able to perform LSUBm calculations for all values $m \leqslant 10$ in both cases. For example, at the LSUB10 level, the number of fundamental configurations that we employ is $N_f = 271\,099$ for the striped AFM state and $N_f = 1\,054\,841$ for the 120° Néel AFM state.

Finally, the only extrapolation that we need to make is to the $m \to \infty$ limit in the LSUBm scheme, where our results for all GS properties are, in principle, exact, since we make no other approximations, and we work from the outset in the thermodynamic ($N \to \infty$) limit. The LSUBm values for the GS energy per spin, $E(m)/N$, converge very rapidly with increasing values of m. We use the extrapolation scheme

$$E(m)/N = a_0 + a_1 m^{-2} + a_2 m^{-4}, \quad (15)$$

which has been very widely tested and found to apply for a large variety of spin-lattice model [29,31,58–81]. As is to be expected, the expectation values of other GS quantities converge less rapidly than the energy. For example, for most models studied previously that are either unfrustrated or contain only moderate amounts of frustration, the magnetic order parameter, M, defined in the local spin-coordinate frames by Eq. (14), typically follows a scheme with leading exponent $1/m$ [29,63–65,69,71,72],

$$M(m) = b_0 + b_1 m^{-1} + b_2 m^{-2}. \quad (16)$$

On the other hand, for systems close to a QCP or when the magnetic order parameter of the particular phase being studied is either zero or close to zero, the extrapolation scheme of Eq. (16) fits less well. In such cases it typically overestimates the amount of order present. It usually also yields a somewhat too large value of the critical strength of the frustration interaction that is the primary driver for the corresponding phase transition. An alternative extrapolation scheme with leading exponent $1/m^{1/2}$,

$$M(m) = c_0 + c_1 m^{-1/2} + c_2 m^{-3/2}, \quad (17)$$

has then been found both to provide an excellent fit to the LSUBm results for a wide variety of models [59,61,68,70,73–80] and also to yield more accurate values of the corresponding QCP. In practice, any of the extrapolation formulas of Eqs. (15)–(17), each of which contains three fitting parameters, is ideally fitted to LSUBm results with at least four different values of m, in order to obtain accurate and robust fits. In so far as there is no conflict with this fitting rule, the lowest-order results with $m \leqslant 3$ are also excluded, so far as practicable, since these results are usually rather far from the asymptotic regime.

IV. RESULTS

We now present our CCM results for the spin-$\frac{1}{2}$ $J_1 - J_2$ model (with $J_1 \equiv 1$) on the triangular lattice, using both the 120° Néel and the collinear striped AFM states shown in Fig. 1 as model states, and employing the LSUBm truncation scheme in each case for values of the truncation index $m \leqslant 10$. We first display the results for the GS energy per spin, E/N, in Fig. 2. Data are shown both for the "raw" LSUBm results in Fig. 2(a) and for several extrapolations based on Eq. (15) in Fig. 2(b), using different LSUBm data sets.

Several preliminary observations concerning the results shown are in order. First, Fig. 2(a) clearly shows that the GS energy per spin converges quite rapidly as a function of the LSUBm truncation index m for both AFM phases based on the 120° Néel state (left curves) and the striped state (right curves). Second, it is apparent from Fig. 2(a) that there is a marked even-odd staggering effect for the raw LSUBm results based on both model states, which is particularly acute for the striped state. In both cases, however, the difference in the corresponding values for E/N, at a given value of J_2, tends to be smaller between pairs of LSUBm results with $m = \{2n, 2n+1\}$ than between corresponding pairs with

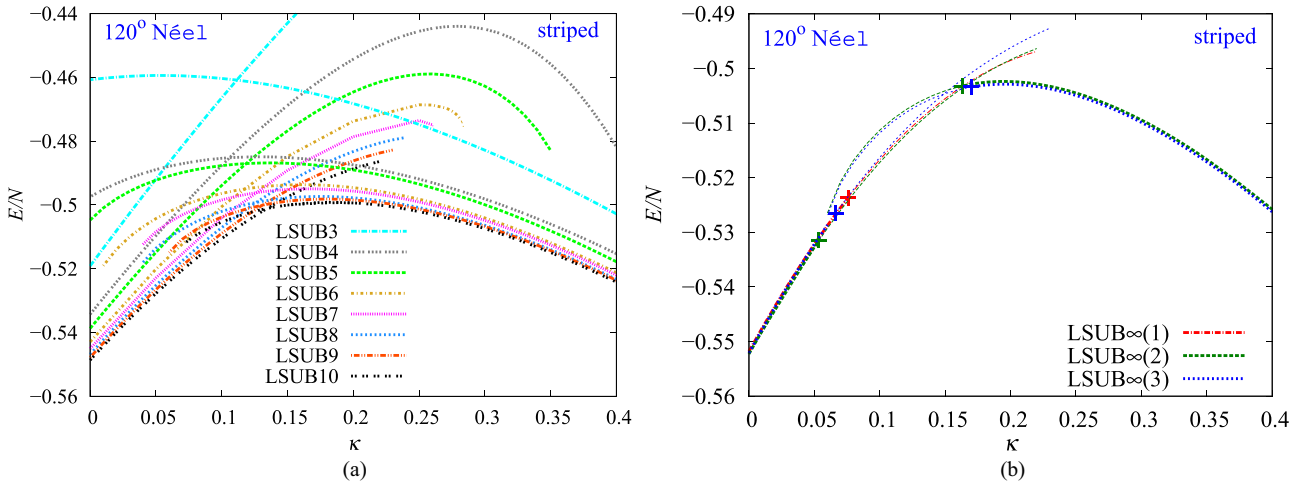

FIG. 2. (Color online) CCM results for the GS energy per spin, E/N, as a function of the frustration parameter $\kappa \equiv J_2/J_1$, for the spin-$\frac{1}{2}$ $J_1 - J_2$ model on the triangular lattice (with $J_1 \equiv +1$). The left curves in each panel are based on the 120° Néel AFM state as CCM model state, while the right curves are similarly based on the striped AFM state as CCM model state. (a) The LSUBm results with $3 \leqslant m \leqslant 10$, shown out to their (approximately determined) termination points. Portions of the curves with thinner lines denote the (approximately determined) unphysical regions where the magnetic order parameter takes negative values ($M < 0$). (b) The corresponding LSUB$\infty(k)$ extrapolations, based on Eq. (15): the $k = 1$ curve for the 120° Néel model state is based on LSUBm results with $m = \{5,6,7,8,9,10\}$, while the $k = \{2,3\}$ curves for both model states are based on LSUBm results with $m = \{4,6,8,10\}$ and $m = \{3,5,7,9\}$, respectively. The plus (+) symbols mark those points where the corresponding extrapolated solutions have vanishing magnetic order parameters, $M = 0$ [and see Fig. 3(b)]. Those sections of the curves beyond the plus (+) symbols, shown with thinner lines, indicate unphysical regions, where $M < 0$ for these approximations (and see text for further details).

$m = \{2n+1, 2n+2\}$, for integral values of n. Third, for a given LSUBm order of approximation, we see from Fig. 2(a) that the corresponding pairs of curves for E/N, based on both model states, cross one another at a value of the frustration parameter κ in the vicinity of the classical transition point at $\kappa_1^{\rm cl} = \frac{1}{8}$. Thus, there is clear preliminary evidence of a quantum phase transition in the $s = \frac{1}{2}$ system from a phase with 120° Néel AFM ordering at low values of κ to one with striped AFM ordering at high values of κ, although it is not yet clear whether there is a direct transition between these phases or whether it occurs via an intermediate state. As we shall see below from a closer look at the extrapolated data, our results are much more consistent with the latter scenario.

Fourth, we note from Fig. 2(a) that both sets of curves, based on each of the model states shown, display termination points at specific values of κ. In the case of the 120° Néel curves the termination points are upper ones, while for the striped curves they are lower ones. In each case the termination points, which themselves depend on the LSUBm truncation used, mark the points beyond which there exist no real solutions to the respective set of CCM equations, corresponding to Eq. (10). As is always the case, we see from Fig. 2(a) that as the truncation index m is increased, and the solution hence becomes more accurate, the range of values of the frustration parameter κ over which the corresponding LSUBm approximations have real solutions decreases. Such CCM termination points have by now been observed in many different spin-lattice problems and are both well documented and well understood (see, e.g., Refs. [58,71]), and are discussed further below. In particular, they provide a clear first signal of the corresponding QCPs in the system under study, which denote the points at which the respective forms of order shown by the model states themselves melt. In practice, however, what one finds is that accurate solutions to the CCM LSUBm equations of Eq. (10) require an increasingly larger amount of computer power the nearer a termination point is approached. To obtain very accurate values of the termination points themselves is thus computationally very costly.

A CCM LSUBm termination point $\kappa_i^t(m)$ always arises at the point where the solution with the ith model state to the corresponding CCM equations given by Eq. (10) becomes complex. Beyond such a point there actually exist two branches of unphysical solutions, which are complex conjugates of one another. Thus, in the region where the solution that tracks the true physical solution is (necessarily) real, there actually exists another real solution, which is numerically unstable and, hence, difficult to find in practice. The physical branch is, luckily, always the numerically stable solution. It is also always easily identifiable in practice as the one that becomes exact in some known limit. In all of our displayed results, therefore, we display with confidence the branch that represents the true (stable) ground state of the system. This physical branch then meets the corresponding unphysical branch at some termination point (typically with infinite slope in curves such as those in Fig. 2), beyond which no real solutions exist and the two solutions branch into the complex plane as conjugate pairs. As the LSUBm truncation index becomes larger, the two branches of real solutions become closer, and as $m \to \infty$ they merge, leaving the termination point as a mathematical branch point, which represents the corresponding quantum critical point. The LSUBm termination points are thus themselves approximations to these critical points. Indeed, their $m \to \infty$ extrapolations may be used as a method to estimate the position of the phase boundary [58]. Both since the LSUBm termination points themselves are computationally costly to obtain accurately, as already noted, and also since we have other more

accurate criteria at our disposal to find the quantum critical points, as we shall see below, we do not use this method here.

What is found here too, in common with many other applications of the CCM to spin-lattice systems, and as we shall discuss more explicitly below when we discuss our corresponding results for the magnetic order parameter M, is that in the vicinity of the LSUBm termination points the respective solutions also become unphysical in the sense that there exists a finite range of values of κ for which M becomes negative. Thus, before the actual termination point of each curve shown in Fig. 2(a), there exists a range of values of κ over which $M < 0$. Such (approximately determined) regions where $M < 0$ are shown in Fig. 2(a) by thinner lines than the corresponding physical regions, where $M > 0$, that are themselves denoted by thicker lines.

It is perhaps worth emphasizing that the regions where $M < 0$ occur both for LSUBm solutions with m finite and for the corresponding LSUB∞ extrapolations. We comment further on these points below when the actual results for M are discussed.

We show in Fig. 2(b) the corresponding extrapolated (LSUB∞) values, a_0, of the GS energy per spin, in each case using Eq. (15) with various LSUBm data sets. In light of the above-mentioned even-odd staggering effect in the raw LSUBm results, we show separately extrapolations using the even-m results $m = \{4,6,8,10\}$ and odd-m results $m = \{3,5,7,9\}$, for both model states. For the case of the 120° Néel AFM model state, for which the staggering is not too pronounced, we also show the extrapolated LSUB∞ results a_0 from Eq. (15) using the data set $m = \{5,6,7,8,9,10\}$. For both model states the various extrapolated results are in excellent agreement with one another.

We note that for both the even-m and odd-m extrapolations we have tested explicitly for the applicability of Eq. (15). Clearly, for any GS physical observable X, one may always check directly for the correct leading exponent ν in the asymptotic ($m \to \infty$) fitting formula,

$$X(m) = x_0 + x_1 m^{-\nu}, \tag{18}$$

by fitting an LSUBm set of results $\{X(m)\}$ to this form, and treating each of the parameters x_0, x_1, and ν as fitting parameters [61,62,64,65,79,80]. For each of the even-m and odd-m data sets used in Fig. 2(b) the exponent ν from fitting to the form of Eq. (18) is very close to the value 2, thereby justifying the use of Eq. (15) in these cases. While the even-odd staggering effect leads to a fit with a comparatively worse value of χ^2 when both even and odd values of m are used together than those obtained using only even values or only odd values of m separately, such fits also yield values of ν close to 2 for the GS energy per spin.

Before turning to our corresponding results for the magnetic order parameter, M, it is worth discussing first the accuracy of our results. In order to do so let us consider the case $\kappa = 0$ for the pure triangular-lattice HAFM. Thus, our extrapolated LSUB∞ results using Eq. (15) are $E(\kappa = 0)/N \approx -0.55227 \pm 0.00011$ with LSUBm results $m = \{4,6,8,10\}$, $E(\kappa = 0)/N \approx -0.55207 \pm 0.00001$ with LSUBm results $m = \{3,5,7,9\}$, and $E(\kappa = 0)/N \approx -0.55180 \pm 0.00033$ with LSUBm results $m = \{5,6,7,8,9,10\}$, and where in each case the errors quoted are solely those associated with the respective fits. A careful analysis of the errors yields our best estimate, $E(\kappa = 0)/N = -0.5521(2)$. This may be compared, for example, with the values $E(\kappa = 0)/N = -0.5502(4)$ from a linked-cluster SE technique [24], $E(\kappa = 0)/N = -0.5415$ [20] and $E(\kappa = 0)/N = -0.5526$ [22] from two separate ED analyses of small clusters of size $N \leqslant 36$ [20,22], $E(\kappa = 0)/N = -0.5458(1)$ from a GFMC technique [26], $E(\kappa = 0)/N = -0.5533$ from a Schwinger-boson mean-field theory (SBMFT) approach with $O(1/N)$ Gaussian fluctuations included [83], and $E(\kappa = 0)/N = -0.5358$ and $E(\kappa = 0)/N = -0.5468$ from leading-order and second-order SWT [7,9], respectively. Our present value may also be compared with the value $E(\kappa = 0)/N = -0.5529$ from a recent CCM analysis [31] of the spin-$\frac{1}{2}$ HAFMs on all 11 Archimedean lattices. Although the raw LSUBm results of this latter work are identical with those obtained here for the $\kappa = 0$ case, the extrapolated value quoted there [31] is based on all results with $4 \leqslant m \leqslant 10$. Due to the even-odd staggering effect present in this case, we believe that the corresponding result $E(\kappa = 0)/N = -0.5529$ is skewed by including unequal numbers of even and odd m values in the fit. Our own result, quoted above, $E(\kappa = 0)/N = -0.5521(2)$, is accordingly more accurate. Finally, it may be worth pointing out that, although, for example, the value $E(\kappa = 0)/N = -0.5533$ cited above from SBMFT lies below our result, the SBMFT method is not variational and hence does not provide a rigorous upper bound to the GS energy.

Figure 3 displays our corresponding results for the GS magnetic order parameter, M, of Eq. (14) to those shown in Fig. 2 for the GS energy per spin, E/N. We see clearly from Fig. 3(a) that at every LSUBm level of approximation the 120° Néel AFM order vanishes at some upper critical value $\kappa_1^c(m)$, while the striped AFM order vanishes at some lower critical value $\kappa_2^c(m)$. These are the respective values used in Fig. 2(a) to demarcate the unphysical regions whose $M < 0$, shown by thinner lines, in the cases where this applies to our data. Once again, the even-odd staggering effect is clearly visible in Fig. 3(a) for the results based on both model states, particularly so for those based on the striped AFM state, for which it is rather striking.

We note that it may not be obvious, *a priori*, why the LSUBm regions with $M < 0$ are necessarily unphysical. Indeed, they could simply arise because the quantization axes have been chosen incorrectly. However, what is found in practice is that the corresponding LSUBm critical values $\kappa_i^c(m)$ converge relatively quickly as $m \to \infty$. Furthermore, the extent of the region between $\kappa_i^c(m)$ and the corresponding LSUBm termination point $\kappa_i^t(m)$, over which $M < 0$, shrinks as m increases. Finally, in the limit, $m \to \infty$, $\kappa_i^c(\infty) = \kappa_i^t(\infty)$, and both thus become equal to the corresponding quantum phase transition point. In this sense, therefore, the unphysical regions in which $M < 0$ are artifacts of LSUBm approximations with finite values of m.

The same LSUBm data sets as were used in Fig. 2(b) for the GS energy per spin extrapolations are also used in Fig. 3(b) for the corresponding extrapolated curves for the GS magnetic order parameter. In all cases the curves have been obtained from the value c_0 using the extrapolation scheme of Eq. (17). Once gain, we have checked explicitly, by first fitting the LSUBm values $M(m)$ of the GS magnetic order parameter

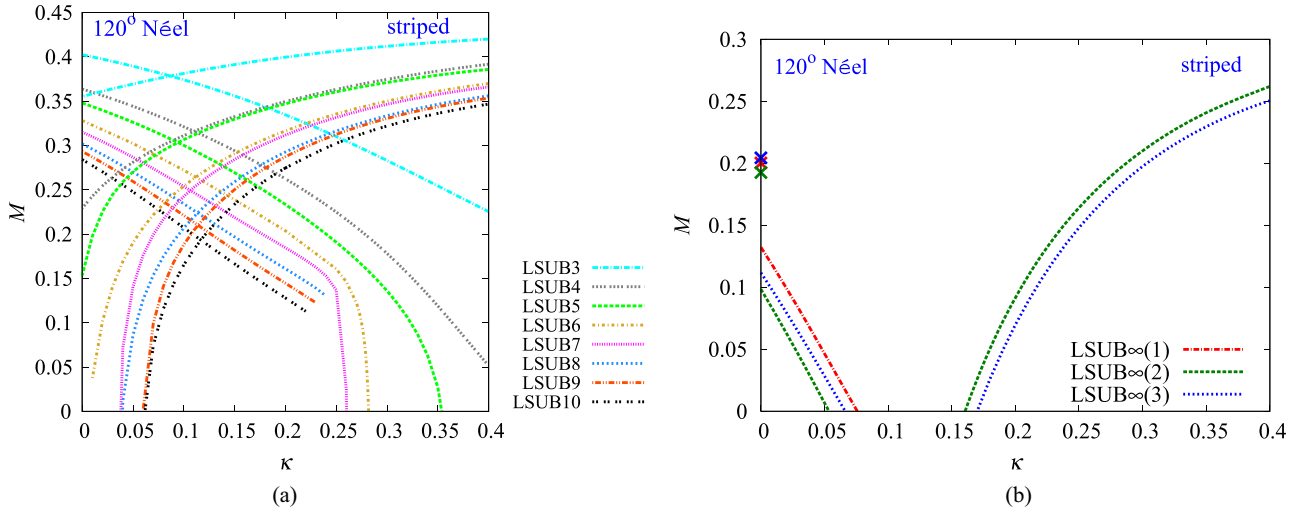

FIG. 3. (Color online) CCM results for the GS magnetic order, M, as a function of the frustration parameter $\kappa = J_2/J_1$, for the spin-$\frac{1}{2}$ $J_1 - J_2$ model on the triangular lattice (with $J_1 > 0$). The left curves in each panel are based on the 120° Néel AFM state as CCM model state, while the right curves are similarly based on the striped AFM state as CCM model state. (a) The LSUBm results with $3 \leqslant m \leqslant 10$, shown out to their (approximately determined) termination points. (b) The corresponding LSUB$\infty(k)$ extrapolations, based on Eq. (17): the $k = 1$ curve for the 120° Néel model state is based on LSUBm results with $m = \{5,6,7,8,9,10\}$, while the $k = \{2,3\}$ curves for both model states are based on LSUBm results with $m = \{4,6,8,10\}$ and $m = \{3,5,7,9\}$, respectively. As explained in the text the extrapolation scheme of Eq. (17) is appropriate for the accurate determination of the QCPs at which $M \to 0$. However, for zero or small dynamic frustration ($J_2 \approx 0$) the scheme of Eq. (16) is appropriate. Rather than crowd the figure with additional full curves based on Eq. (16), we show with cross ($\times$) symbols the corresponding extrapolated values based on the 120° Néel state, using Eq. (16), for the case $\kappa = 0$ only of the triangular-lattice HAFM.

to Eq. (18), that the extrapolation scheme of Eq. (17) is more appropriate than the alternate scheme of Eq. (16) for all of the results based on the striped model state. It is also the case for most of the results based on the 120° Néel model state, especially in the critical regime where $M \to 0$. The only exception is a very narrow region near $\kappa = 0$, where the extrapolation scheme of Eq. (16) is clearly preferred, as has been observed many time before, as discussed in Sec. III.

The corresponding extrapolated values, b_0, obtained for the spin-$\frac{1}{2}$ triangular-lattice HAFM (viz., at $\kappa = 0$) are shown in Fig. 3(b) by the cross symbols. Once again, these values may be used as benchmarks for comparison with those obtained by other methods, and to discuss the overall quality of our CCM results. Our extrapolated LSUB∞ results using Eq. (16) are $M(\kappa = 0) \approx 0.193 \pm 0.002$ based on the data set $m = \{4,6,8,10\}$, $M(\kappa = 0) \approx 0.204 \pm 0.003$ based $m = \{3,5,7,9\}$, and $M(\kappa = 0) \approx 0.200 \pm 0.009$ based $m = \{5,6,7,8,9,10\}$. In each case the quoted error is that associated solely with the quality of the fit. The even-odd staggering effect is the cause of the larger error associated with the fit using both even and odd values of m, compared to those associated with the fits using only even or only odd values of m. A careful analysis of the errors yields our best estimate, $M(\kappa = 0) = 0.198(5)$.

This value may again be compared with the corresponding value $M(\kappa = 0) = 0.187$ from another recent CCM analysis [31] of the spin-$\frac{1}{2}$ HAFMs on all 11 Archimedean lattices. As discussed above for the GS energy per spin results, although this latter work obtained raw LSUBm results for the triangular-lattice HAFM that are identical to our own $\kappa = 0$ results, and although it also employed the extrapolation scheme of Eq. (16), the result quoted is based on using the data set $m = \{4,5,6,7,8,9,10\}$. Both the even-odd staggering effect itself and the fact that the extrapolation is now based on unequal numbers of even and odd m values used in the fit now conspire to make the obtained value of 0.187 less accurate than the value quoted here, 0.198(5).

Our value may again be compared with those from using the best of the available alternate methods. For example, a linked-cluster SE analysis [24] yields the value $M(\kappa = 0) = 0.19(2)$; a recent ED analysis [22] of small clusters of size $N \leqslant 36$ yields the $N \to \infty$ extrapolated value $M(\kappa = 0) = 0.193$; a GFMC technique [26] based on clusters of size $N \leqslant 144$ yields the $N \to \infty$ extrapolated value $M(\kappa = 0) = 0.205(10)$; and a DMRG analysis [25] yields the $N \to \infty$ extrapolated value $M(\kappa = 0) = 0.205(15)$. All of these modern values are seen to be in excellent agreement with one another, with our own CCM result being now perhaps the most accurate available. By contrast, the results from SWT and SBMFT are significantly larger. Thus, the corresponding values from leading-order and second-order SWT [7,9] are $M(\kappa = 0) = 0.2387$ and $M(\kappa = 0) = 0.2497$, respectively, while the result from (lowest-order) SBMFT [46] is $M(\kappa = 0) = 0.275$.

The LSUB∞ extrapolated curves for M shown in Fig. 3(b) use the extrapolation scheme of Eq. (17). This scheme is particularly appropriate in the quantum critical regimes, where M becomes vanishingly small, as we have again explicitly checked by first finding the leading exponent ν in fits of M to the scheme of Eq. (18), using various LSUBm data sets. The corresponding values where $M \to 0$ are the values shown in Fig. 2(b) on the extrapolated GS energy per spin curves by the plus (+) symbols. They provide our best estimates for the QCPs, $\kappa_1^c \equiv \kappa_1^c(\infty)$ at which the 120° Néel AFM order melts and $\kappa_2^c \equiv \kappa_2^c(\infty)$ at which the striped AFM order melts. We find the explicit estimate $\kappa_1^c \approx 0.053$ from the LSUB∞

extrapolation scheme of Eq. (17) using the LSUBm data set $m = \{4,6,8,10\}$, with the corresponding estimate $\kappa_1^c \approx 0.066$ from comparably using the data set $m = \{3,5,7,9\}$. The estimate obtained from using the data set $m = \{5,6,7,8,9,10\}$ is $\kappa_1^c \approx 0.076$, although the quality of this fit is considerably worse than those using only even or only odd values of m, due to the even-odd staggering effect discussed above, and hence this latter value comes with an appreciably larger error. The corresponding estimates obtained for κ_2^c are $\kappa_2^c \approx 0.163$ from using the LSUBm data set $m = \{4,6,8,10\}$, and $\kappa_2^c \approx 0.170$ from using the set of $m = \{3,5,7,9\}$. On the basis of an analysis of all our results our best estimates for the two QCPs are $\kappa_1^c \approx 0.060(10)$ and $\kappa_2^c \approx 0.165(5)$.

In the concluding section we now summarize and discuss our results.

V. SUMMARY AND DISCUSSION

We have studied the spin-$\frac{1}{2}$ $J_1 - J_2$ model on the triangular lattice using the CCM in the case of AFM NN bonds ($J_1 > 0$) and AFM NNN bonds ($J_2 \equiv \kappa J_1 < 0$), in the range $0 \leqslant \kappa \leqslant 1$ for the frustration parameter. A big advantage of the CCM is that, unlike most alternative accurate methods, we work from the outset in the thermodynamic limit ($N \to \infty$) of an infinite lattice, which hence obviates the need for any finite-size scaling.

For the limiting case $\kappa = 0$ of the triangular-lattice HAFM with NN bonds only we find, in agreement with most other recent high-order calculations, that the quantum $s = \frac{1}{2}$ model is magnetically ordered, retaining the classical ($s \to \infty$) 120° Néel AFM order, albeit with a reduced value of the GS magnetic order parameter M (viz., the local on-site magnetization), $M = 0.198(5)$, compared to the classical value $M = 0.5$. In the same $\kappa = 0$ limit the GS energy per spin is found to be $E/N = -0.5521(2)$. Both values are in excellent agreement with those from other recent studies using high-accuracy methods, and both possibly now represent the most accurate values available.

In the classical ($s \to \infty$) $J_1 - J_2$ model on the triangular lattice the 120° Néel AFM state is the stable GS phase in the region $0 \leqslant \kappa \leqslant \kappa_1^{\rm cl}$, where $\kappa_1^{\rm cl} = \frac{1}{8}$. At $\kappa = \kappa_1^{\rm cl}$ there is then a first-order phase transition to an IDF of 4-sublattice Néel states, which form the stable GS in the region $\kappa_1^{\rm cl} < \kappa < \kappa_2^{\rm cl}$, where $\kappa_2^{\rm cl} = 1$. Lowest-order SWT and ED calculations on finite clusters show that from this IDF of states, the 2-sublattice striped states are energetically preferred over the entire region $\frac{1}{8} < \kappa < 1$. In the light of these findings we have applied the CCM to the spin-$\frac{1}{2}$ $J_1 - J_2$ model on the triangular lattice, using both the 3-sublattice 120° Néel and 2-sublattice striped AFM states as model states.

It is worth noting that, in principle, we could easily use other candidate states from the IDF of 4-sublattice Néel states as CCM model states, apart from the striped state used here. By comparing their extrapolated (LSUB∞) GS energies we could then use the CCM itself to provide evidence for a quantum order-by-disorder selection of the striped state among the classical IDF. However, since many other methods provide strong evidence of the striped state being selected, it seems somewhat redundant to do so. Furthermore, for the actual calculation of the QCP at κ_2^c, at which quasiclassical ordering reappears for all $\kappa > \kappa_2^c$, it almost certainly suffices to use any of the IDF as a CCM model state.

Calculations have been performed in the well-defined LSUBm hierarchy of approximations, which becomes exact in the limit $m \to \infty$. High-order calculations have been carried out for both quasiclassical states for values of the truncation index $m \leqslant 10$, and we have discussed the extrapolations to the $m \to \infty$ limit for both the GS energy per spin, E/N, and the GS magnetic order parameter, M.

Our main finding is that the classical phase transition at $\kappa_1^{\rm cl} = \frac{1}{8}$ is split, for the spin-$\frac{1}{2}$ version of the model, into two quantum phase transitions at $\kappa_1^c < \kappa_1^{\rm cl}$ and $\kappa_2^c > \kappa_1^{\rm cl}$. The quasiclassical 120° Néel AFM order persists now only over the diminished range $(0 <) \kappa < \kappa_1^c$ under study, while the quasiclassical striped AFM order persists over the (also diminished) range $\kappa_2^c < \kappa$ (< 1) under study. Our best estimates for the two spin-$\frac{1}{2}$ QCPs are $\kappa_1^c = 0.060(10)$ and $\kappa_2^c = 0.165(5)$.

These findings may be compared with the corresponding results from other methods. For example, lowest-order (or linear) SWT [48] predicts a quantum nonmagnetic phase for the spin-$\frac{1}{2}$ case in the range $0.10 \lesssim \kappa \lesssim 0.14$. However, when leading-order, $O(1/s^2)$, corrections are included [42,47] this window closes and the prediction then is that there is a direct first-order transition at $\kappa \approx \frac{1}{8}$ between the two quasiclassical phases for the $s = \frac{1}{2}$ case, just as for the classical ($s \to \infty$) case. By contrast, lowest-order SBMFT [46] predicts a first-order direct transition for the spin-$\frac{1}{2}$ model between the two quasiclassical states at some critical value $\kappa^c \approx 0.16$, with no interesting disordered phase. At this critical point the order parameter M is reduced from its value $M(\kappa = 0) = 0.275$, but is still nonzero, $M(\kappa \approx 0.16) \approx 0.17$. Now, however, when the leading-order corrections due to Gaussian fluctuations are included [50] in the SBMFT approach, there opens a window $0.12 \lesssim \kappa \lesssim 0.19$, where the spin stiffness vanishes and the quasiclassical 120° Néel and striped forms of magnetic LRO both melt. Clearly, the results of SWT and SBMFT approaches are in conflict with one another.

Very recently, the phase diagram of the spin-$\frac{1}{2}$ $J_1 - J_2$ model on the triangular lattice has been studied using the variational Monte Carlo (VMC) method within various broad classes of trial many-body wave functions [51,52]. In a first study [51], Mishmash *et al.* compared the energies of the two quasiclassical AFM states, as modeled by Jastrow-type wave functions, of the form pioneered by Huse and Elser [10], which incorporate NN and NNN correlations only, with that of a class of trial spin-liquid states with d-wave symmetry. On the basis of such a VMC calculation they find QCPs at $\kappa_1^c \approx 0.05$ above which the 120° Néel AFM order melts, and $\kappa_2^c \approx 0.18$ below which the striped AFM order melts. In between they find that a QSL state with nodal d-wave symmetry has lower energy than either of the surrounding quasiclassical states. Clearly, the values so obtained for the positions of the two QCPs are in good agreement with those obtained in the present study.

Nevertheless, the Jastrow-type trial variational wave functions used by Mishmash *el*. [51] are relatively inaccurate. For example, for the case $\kappa = 0$, Huse and Elser [10] obtained a VMC upper-bound value for the GS energy per spin of $E(\kappa = 0)/N \approx -0.5367$ with a trial wave function (probably)

containing more free parameters than that used by Mishmash *et al.* for the 120° Néel AFM state, which is appreciably above both our own value of $E(\kappa = 0)/N = -0.5521(2)$ and those from other accurate high-order methods quoted previously. Although the difference in energy values may seem small, we note that the classical value of the energy per spin is -0.375 from Eq. (2). Thus the best Jastrow-type wave function of Huse and Elser, which included *all* two-spin interactions with a spin-Jastrow factor proportional to $r_{ij}^{-\sigma}$, where r_{ij} is the Euclidean distance between sites i and j, together with only the shortest-range three-spin term, still gives only about 92% of the nontrivial quantum part of the GS energy. Since the energy differences between competing phases are themselves small, as may be seen explicitly from Fig. 2(b), such errors may be highly significant.

Indeed, the authors of a more recent VMC calculation [52] believe that the calculations of Mishmash *et al.* may intrinsically overestimate the QSL phase, due to the relative inaccuracy of their trial spin-Jastrow wave functions for the quasiclassical AFM states. Instead, Kaneko *et al.* [52] calculate the ground and low-lying excited states of the spin-$\frac{1}{2}$ $J_1 - J_2$ model on the triangular lattice using a many-variable VMC approach. They again find three locally stable states as candidates for the GS phase. These once more include the 120° Néel AFM state and the striped AFM state, now together with a QSL state (with no LRO order) of an unconventional critical (algebraic) type, characterized by gapless excitations and a power-law decay of the spin-spin correlation function. Within their (enlarged) class of trial wave functions, Kaneko *et al.* find that the 120° Néel AFM state is favored for values $\kappa < \kappa_1^c = 0.10(1)$, the striped AFM state is favored for values $\kappa > \kappa_2^c = 0.135(5)$, with the critical QSL forming the stable GS phase for $\kappa_1^c < \kappa < \kappa_2^c$.

Clearly, all variational studies are restricted by the class of trial wave functions that they employ. For that reason quantitative estimates obtained from them for QCPs or phase boundaries must always be treated with extreme caution. What they can reveal, however, is when certain states (e.g., of a QSL variety) become competitive energetically with other more conventional (e.g., quasiclassical) states.

One strength of the CCM used here is that it is certainly capable of giving accurate values of QCPs and phase boundaries. For that reason we tend to believe that our own values for κ_1^c and κ_2^c are intrinsically more accurate than those coming from VMC calculations. On the other hand, a weakness of the CCM as implemented so far is that, despite giving accurate values of the QCPs at which the two forms of quasiclassical order melt, our calculation to date gives no information about the nature of the intermediate state.

Indeed, each of the CCM model states used here has been of the independent spin-product type. While it is certainly true that solutions of the CCM are, to some extent, always tied to these reference states, the relationship can be quite subtle. For example, it has been shown explicitly [84] that exact valence-bond crystal (VBC) states of the local dimer or plaquette variety can also be described exactly within the CCM, starting from the use of collinear independent-spin product states as model states. More mundanely, one may also describe non-classical VBC ordering within the CCM by the direct employment of valence-bond model states [85] (e.g., on the square lattice, two- or four-spin singlet product states) in place of the simpler single-spin product states used here. A complication of this approach, however, is that a whole new matrix-operator formalism then needs to be created for each new problem. Both the Hamiltonian and the CCM bra- and ket-state operators must then be rewritten in terms of the new matrix algebra. Once the commutation relations between the operators have been found, the CCM equations must finally be derived and solved. Although the whole procedure is formally straightforward, its implementation in practice can be both tedious and computationally intensive. What is certainly much more difficult, however, is to use directly a CCM model state of any of the usual QSL types. Indeed, to date, this has never been achieved.

ACKNOWLEDGMENT

We thank the University of Minnesota Supercomputing Institute for the grant of supercomputing facilities.

[1] N. D. Mermin and H. Wagner, Phys. Rev. Lett. **17**, 1133 (1966).
[2] P. W. Anderson, Mater. Res. Bull. **8**, 153 (1973).
[3] P. Fazekas and P. W. Anderson, Philos. Mag. **30**, 423 (1974).
[4] T. Oguchi, J. Phys. Soc. Jpn. Suppl. **52**, 183 (1983).
[5] H. Nishimori and S. J. Miyake, Prog. Theor. Phys. **73**, 18 (1985).
[6] Th. Jolicoeur and J. C. Le Guillou, Phys. Rev. B **40**, 2727(R) (1989).
[7] S. J. Miyake, J. Phys. Soc. Jpn. **61**, 983 (1992).
[8] A. V. Chubukov, S. Sachdev, and T. Senthil, J. Phys.: Condens. Matter **6**, 8891 (1994).
[9] A. L. Chernyshev and M. E. Zhitomirsky, Phys. Rev. B **79**, 144416 (2009).
[10] D. A. Huse and V. Elser, Phys. Rev. Lett. **60**, 2531 (1988).
[11] P. Sindzingre, P. Lecheminant, and C. Lhuillier, Phys. Rev. B **50**, 3108 (1994).
[12] T. Oguchi, H. Nishimori, and Y. Taguchi, J. Phys. Soc. Jpn. **55**, 323 (1986).
[13] V. Kalmeyer and R. B. Laughlin, Phys. Rev. Lett. **59**, 2095 (1987).
[14] K. Yang, L. K. Warman, and S. M. Girvin, Phys. Rev. Lett. **70**, 2641 (1993).
[15] S. Fujiki and D. D. Betts, Can. J. Phys. **65**, 76 (1987).
[16] S. Fujiki, Can. J. Phys. **65**, 489 (1987).
[17] H. Nishimori and H. Nakanishi, J. Phys. Soc. Jpn. **57**, 626 (1988); **58**, 2607 (1989); **58**, 3433 (1989).
[18] M. Imada, J. Phys. Soc. Jpn. **56**, 311 (1987); **58**, 2650 (1989).
[19] P. W. Leung and K. J. Runge, Phys. Rev. B **47**, 5861 (1993).
[20] B. Bernu, P. Lecheminant, C. Lhuillier, and L. Pierre, Phys. Rev. B **50**, 10048 (1994).
[21] B. Bernu, C. Lhuillier, and L. Pierre, Phys. Rev. Lett. **69**, 2590 (1992).
[22] J. Richter, J. Schulenburg, and A. Honecker, in *Quantum Magnetism*, Lecture Notes in Physics, Vol. 645, edited by

U. Schollwöck, J. Richter, D. J. J. Farnell, and R. F. Bishop (Springer-Verlag, Berlin, 2004), p. 85.
[23] R. R. P. Singh and D. A. Huse, Phys. Rev. Lett. **68**, 1766 (1992).
[24] W. Zheng, J. O. Fjærestad, R. R. P. Singh, R. H. McKenzie, and R. Coldea, Phys. Rev. B **74**, 224420 (2006).
[25] S. R. White and A. L. Chernyshev, Phys. Rev. Lett. **99**, 127004 (2007).
[26] L. Capriotti, A. E. Trumper, and S. Sorella, Phys. Rev. Lett. **82**, 3899 (1999).
[27] M. Boninsegni, Phys. Rev. B **52**, 15304 (1995).
[28] C. Zeng, D. J. J. Farnell, and R. F. Bishop, J. Stat. Phys. **90**, 327 (1998).
[29] D. J. J. Farnell, R. F. Bishop, and K. A. Gernoth, Phys. Rev. B **63**, 220402(R) (2001).
[30] S. E. Krüger, R. Darradi, J. Richter, and D. J. J. Farnell, Phys. Rev. B **73**, 094404 (2006).
[31] D. J. J. Farnell, O. Götze, J. Richter, R. F. Bishop, and P. H. Y. Li, Phys. Rev. B **89**, 184407 (2014).
[32] Y. Shirata, H. Tanaka, A. Matsuo, and K. Kindo, Phys. Rev. Lett. **108**, 057205 (2012).
[33] T. Susuki, N. Kurita, T. Tanaka, H. Nojiri, A. Matsuo, K. Kindo, and H. Tanaka, Phys. Rev. Lett. **110**, 267201 (2013).
[34] R. Coldea, D. A. Tennant, A. M. Tsvelik, and Z. Tylczynski, Phys. Rev. Lett. **86**, 1335 (2001).
[35] T. Ono, H. Tanaka, H. Aruga Katori, F. Ishikawa, H. Mitamura, and T. Goto, Phys. Rev. B **67**, 104431 (2003).
[36] N. A. Fortune, S. T. Hannahs, Y. Yoshida, T. E. Sherline, T. Ono, H. Tanaka, and Y. Takano, Phys. Rev. Lett. **102**, 257201 (2009).
[37] J. Villain, J. Phys. (France) **38**, 385 (1977); J. Villain, R. Bidaux, J.-P. Carton, and R. Conte, *ibid.* **41**, 1263 (1980).
[38] Th. Jolicoeur, E. Dagotto, E. Gagliano, and S. Bacci, Phys. Rev. B **42**, 4800(R) (1990).
[39] S. E. Korshunov, J. Phys. C **19**, 5927 (1986).
[40] C. L. Henley, J. Appl. Phys. **61**, 3962 (1987).
[41] A. V. Chubukov and D. I. Golosov, J. Phys.: Condens. Matter **3**, 69 (1991).
[42] A. V. Chubukov and T. Jolicoeur, Phys. Rev. B **46**, 11137 (1992).
[43] S. E. Korshunov, Phys. Rev. B **47**, 6165 (1993).
[44] P. Lecheminant, B. Bernu, C. Lhuillier, and L. Pierre, Phys. Rev. B **52**, 6647 (1995).
[45] G. Baskaran, Phys. Rev. Lett. **63**, 2524 (1989).
[46] C. J. Gazza and H. A. Ceccatto, J. Phys.: Condens. Matter **5**, L135 (1993).
[47] R. Deutscher and H. U. Everts, Z. Phys. B **93**, 77 (1993).
[48] N. B. Ivanov, Phys. Rev. B **47**, 9105 (1993).
[49] P. Sindzingre, B. Bernu, and P. Lecheminant, J. Phys.: Condens. Matter **7**, 8805 (1995).
[50] L. O. Manuel and H. A. Ceccatto, Phys. Rev. B **60**, 9489 (1999).
[51] R. V. Mishmash, J. R. Garrison, S. Bieri, and C. Xu, Phys. Rev. Lett. **111**, 157203 (2013).
[52] R. Kaneko, S. Morita, and M. Imada, J. Phys. Soc. Jpn. **83**, 093707 (2014).
[53] R. F. Bishop and H. G. Kümmel, Phys. Today **40**(3), 52 (1987).
[54] J. S. Arponen and R. F. Bishop, Ann. Phys. (N.Y.) **207**, 171 (1991).
[55] R. F. Bishop, J. B. Parkinson, and Yang Xian, Phys. Rev. B **44**, 9425 (1991).
[56] R. F. Bishop, Theor. Chim. Acta **80**, 95 (1991).
[57] R. F. Bishop, in *Microscopic Quantum Many-Body Theories and Their Applications*, Lecture Notes in Physics, Vol. 510, edited by J. Navarro and A. Polls (Springer-Verlag, Berlin, 1998), p. 1.
[58] D. J. J. Farnell and R. F. Bishop, in *Quantum Magnetism*, Lecture Notes in Physics, Vol. 645, edited by U. Schollwöck, J. Richter, D. J. J. Farnell, and R. F. Bishop (Springer-Verlag, Berlin, 2004), p. 307.
[59] R. F. Bishop, P. H. Y. Li, R. Darradi, J. Schulenburg, and J. Richter, Phys. Rev. B **78**, 054412 (2008).
[60] R. F. Bishop, P. H. Y. Li, D. J. J. Farnell, and C. E. Campbell, J. Phys.: Condens. Matter **24**, 236002 (2012).
[61] R. F. Bishop, P. H. Y. Li, and C. E. Campbell, J. Phys.: Condens. Matter **25**, 306002 (2013).
[62] R. F. Bishop, P. H. Y. Li, and C. E. Campbell, Phys. Rev. B **89**, 214413 (2014).
[63] S. E. Krüger, J. Richter, J. Schulenburg, D. J. J. Farnell, and R. F. Bishop, Phys. Rev. B **61**, 14607 (2000).
[64] R. F. Bishop, D. J. J. Farnell, S. E. Krüger, J. B. Parkinson, J. Richter, and C. Zeng, J. Phys.: Condens. Matter **12**, 6887 (2000).
[65] R. Darradi, J. Richter, and D. J. J. Farnell, Phys. Rev. B **72**, 104425 (2005).
[66] D. Schmalfuß, R. Darradi, J. Richter, J. Schulenburg, and D. Ihle, Phys. Rev. Lett. **97**, 157201 (2006).
[67] R. Darradi, O. Derzhko, R. Zinke, J. Schulenburg, S. E. Krüger, and J. Richter, Phys. Rev. B **78**, 214415 (2008).
[68] R. F. Bishop, P. H. Y. Li, R. Darradi, and J. Richter, J. Phys.: Condens. Matter **20**, 255251 (2008).
[69] R. F. Bishop, P. H. Y. Li, D. J. J. Farnell, and C. E. Campbell, Phys. Rev. B **79**, 174405 (2009).
[70] J. Richter, R. Darradi, J. Schulenburg, D. J. J. Farnell, and H. Rosner, Phys. Rev. B **81**, 174429 (2010).
[71] R. F. Bishop, P. H. Y. Li, D. J. J. Farnell, and C. E. Campbell, Phys. Rev. B **82**, 024416 (2010).
[72] R. F. Bishop, P. H. Y. Li, D. J. J. Farnell, and C. E. Campbell, Phys. Rev. B **82**, 104406 (2010).
[73] J. Reuther, P. Wölfle, R. Darradi, W. Brenig, M. Arlego, and J. Richter, Phys. Rev. B **83**, 064416 (2011).
[74] D. J. J. Farnell, R. F. Bishop, P. H. Y. Li, J. Richter, and C. E. Campbell, Phys. Rev. B **84**, 012403 (2011).
[75] O. Götze, D. J. J. Farnell, R. F. Bishop, P. H. Y. Li, and J. Richter, Phys. Rev. B **84**, 224428 (2011).
[76] R. F. Bishop, P. H. Y. Li, D. J. J. Farnell, J. Richter, and C. E. Campbell, Phys. Rev. B **85**, 205122 (2012).
[77] P. H. Y. Li, R. F. Bishop, D. J. J. Farnell, and C. E. Campbell, Phys. Rev. B **86**, 144404 (2012).
[78] P. H. Y. Li, R. F. Bishop, C. E. Campbell, D. J. J. Farnell, O. Götze, and J. Richter, Phys. Rev. B **86**, 214403 (2012).
[79] P. H. Y. Li, R. F. Bishop, and C. E. Campbell, Phys. Rev. B **88**, 144423 (2013).
[80] R. F. Bishop, P. H. Y. Li, and C. E. Campbell, Phys. Rev. B **88**, 214418 (2013).
[81] P. H. Y. Li, R. F. Bishop, and C. E. Campbell, Phys. Rev. B **89**, 220408(R) (2014).
[82] We use the program package CCCM of D. J. J. Farnell and J. Schulenburg; see http://www-e.uni-magdeburg.de/jschulen/ccm/index.html.
[83] L. O. Manuel, A. E. Trumper, and H. A. Ceccatto, Phys. Rev. B **57**, 8348 (1998).
[84] D. J. J. Farnell, J. Richter, R. Zinke, and R. F. Bishop, J. Stat. Phys. **135**, 175 (2009).
[85] Y. Xian, J. Phys.: Condens. Matter **6**, 5965 (1994).